Advanced Heat Resistant Steel for Power Generation, eds R. Viswanathan and J. Nutting, Institute of Materials, London, 1998, pp. 223-233.

Precipitation Reactions In 3Cr1.5Mo Power Plant Steel

Nobuhiro Fujita and H. K. D. H. Bhadeshia
Department of Materials Science and Metallurgy, University of Cambridge

ABSTRACT

A method has recently been developed to estimate the speed with which precipitation reactions occur in power plant steels. It is based on Avrami theory but with an adaptation that allows the treatment of simultaneous reactions. A number of approximations and inconsistencies in the theory have been eliminated in the present work. The modified theory is shown to successfully predict new experimental data on 3Cr1.5Mo steel.

1. INTRODUCTION

Steels for use at elevated temperature rely on a variety of precipitates for their resistance to creep deformation. The precipitation process in the vast majority of creep-resistant steels occurs in a complicated manner, beginning with phases which are easy to nucleate but which are metastable. It is only after prolonged aging (e.g. many decades at 600 °C) that the equilibrium phase mixture might be obtained. This is just as well because the equilibrium microstructure is unlikely to be useful in creep applications.

Steels destined for power plant applications might contain any of the following precipitates: iron base carbides or carbonitrides (M_3C, $M_{2.4}C$ etc.), M_2C, M_7C_3, $M_{23}C_6$, M_5C_2, M_6C, graphite and Laves phase. It is obviously difficult to design a steel with specific particles in mind given the complexity of the precipitation events. A theory has recently been proposed (Robson and Bhadeshia [1, 2]; Jones and Bhadeshia [3]) which adapts the classical Avrami [4-8] model to enable simultaneous precipitation reactions to be tackled. Although this new theory has been applied to power plant steels, it has only been tested against limited data and it contains a number of important approximations, some of which may not be generally valid. The purpose of the present work was firstly to make the theory more rigorous in its application, and secondly, to test the model against some critical new experimental data for 3Cr1.5Mo steel.

2. EXPERIMENTAL PROCEDURE

The 3Cr1.5Mo (Table I) steel studied in this work was vacuum-melted as a 15 kg ingot, heated at 1250 °C for 30 minutes in an argon atmosphere, hot-rolled to 15 mm thick plate and quenched from a finishing temperature of about 900 °C. Specimens of 3 and 8 mm diameter were then machined and sealed in silica tubes under a partial pressure of argon (about 150 mm Hg) to prevent decarburisation and oxidation. Phase diagram calculations using MTDATA [9] predicted that only austenite is present above 1200 °C in 3Cr1.5Mo steel. Therefore, the

samples were homogenised at 1250 °C for 3 days followed by water quenching to produce a martensitic microstructure. The specimens were then sealed again and tempered at 600 °C for times up to 1000 h, and then quenched into water.

The microstructures were characterised using optical and transmission electron microscopy (TEM), the latter using carbon extraction replicas. Electrolytically extracted residues were analysed using X-rays.

The number densities of precipitates were determined using the method of Ashby and Ebeling [10]. The particle sizes were determined by averaging at least 100 measurements in each case.

Table I: Concentration in wt% of the major alloying elements in 3Cr1.5Mo steel

	C	Mn	Cr	Mo
3Cr1.5Mo	0.10	0.98	2.98	1.50

3. RESULTS

3.1 Microstructural observations

The microstructure of 3Cr1.5Mo following heat treatment at 1250 °C for 3 days followed by water quenching was martensitic.

When the specimen was tempered at 600 °C for 0.05 h (Fig. 1), only M_3C could be detected and most particles appeared to be in the form of plates. Figs. 2 to 4 show a set of transmission electron micrographs and associated diffraction analysis for 3Cr1.5Mo samples tempered for 0.7, 10 and 100 h respectively. M_7C_3 started to precipitate at 0.7 h (Fig. 2). As shown in Fig. 3, at 10 h, the M_3C particles are smaller than was at the case after 0.05 h, implying that they had started dissolving. A small amount of M_3C persisted in the microstructure even after 10 h of heat treatment at 600 °C. As the tempering time was increased to 100 h, M_2C needles and $M_{23}C_6$ particles were clearly observed (Fig. 4).

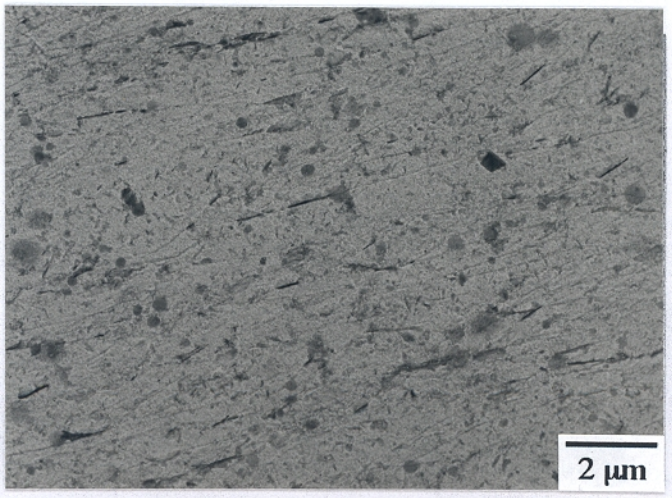

Figure 1: Transmission electron micrograph of 3Cr1.5Mo steel tempered at 600 °C for 0.05 h.

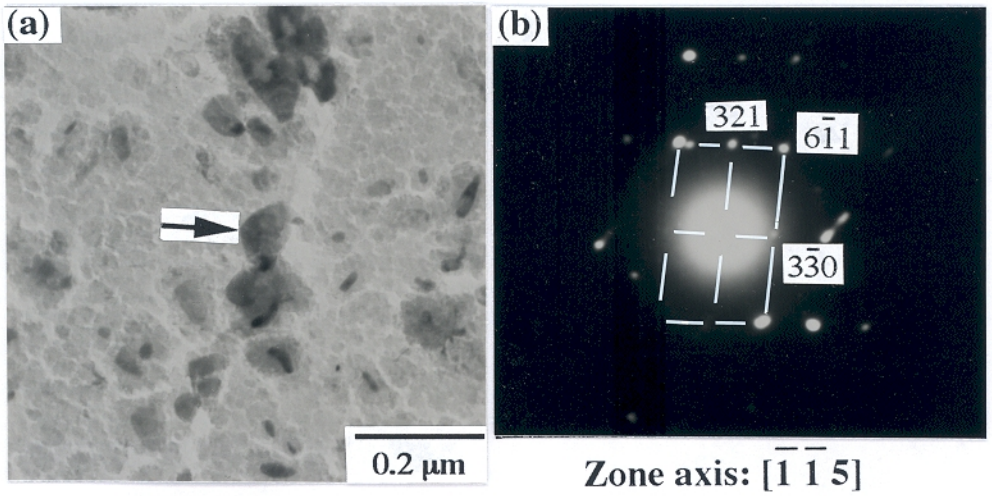

Figure 2: Transmission electron micrograph for 3Cr1.5Mo steel tempered at 600 °C for 0.7 h, (a) image of M_7C_3 particle and (b) electron diffraction pattern from M_7C_3. The arrow in (a) indicates the particle from which the electron diffraction pattern was obtained. In the diffraction pattern, there were streaks characteristic of M_7C_3 [11].

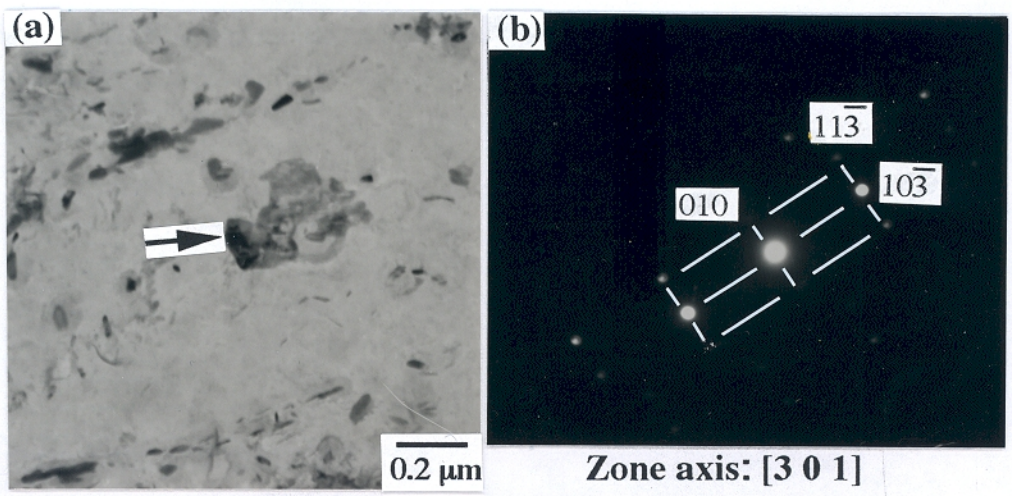

Figure 3: Transmission electron micrograph of 3Cr1.5Mo steel tempered at 600 °C for 10 h, (a) image of M_3C particle and (b) electron diffraction pattern from M_3C. The arrow in (a) indicates the particle from which the electron diffraction pattern was obtained.

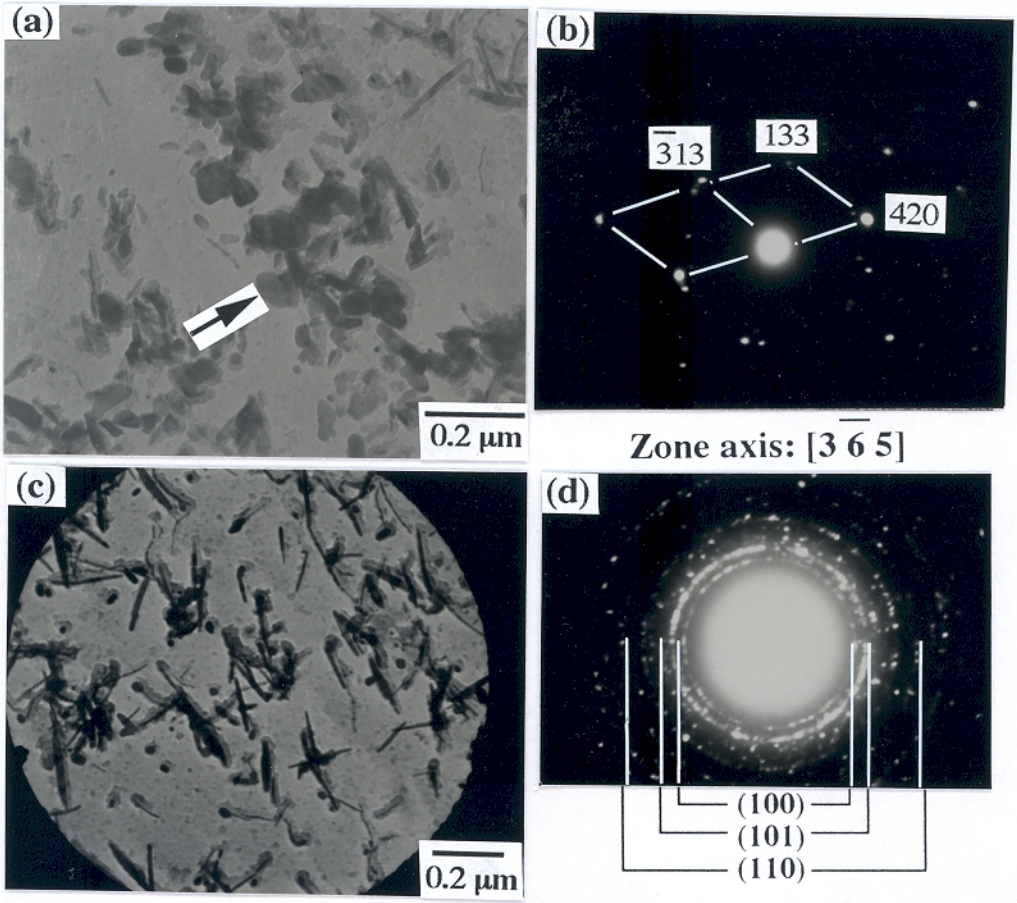

Figure 4: Transmission electron micrograph of 3Cr1.5Mo steel tempered at 600 °C for 100 h, (a) image of $M_{23}C_6$ particle and (b) electron diffraction pattern from $M_{23}C_6$, (c) image of M_2C particles and (d) electron diffraction ring pattern from an array of M_2C particles. The arrow in (a) indicates the particle from which the electron diffraction pattern was obtained.

3.2 X-ray analysis and precipitation sequences

Table II shows a summary of X-ray analysis results of electrolytically extracted residues.

Table II: The results of X-ray analysis for extracted residues of 3Cr1.5Mo steel tempered at 600 °C (VS, S, W and VW mean very strong, strong, weak and very weak X-ray intensities, respectively).

Tempering condition	Precipitates detected			
	M_3C	M_2C	M_7C_3	$M_{23}C_6$
1250 °C - 3 days normalised	W			
600 °C - 0.05 h tempered	W			
600 °C - 0.3 h tempered	VS		W	
600 °C - 0.7 h tempered	VS	VW	S	
600 °C - 10 h tempered	S	W	S	W
600 °C - 100 h tempered	W	S	S	S

The results of both TEM and X-ray analysis are in good agreement. M_2C followed the formation of M_7C_3 which occurred at 0.3 h of tempering. Between 10 h and 100 h tempering, $M_{23}C_6$ was clearly detected and the X-ray intensity from M_3C decreased. This implied the beginning of M_3C dissolution. According to both TEM observations and X-ray analysis of extracted residues, the precipitation sequences at 600 °C for 3Cr1.5Mo steel can be summarised as follows:

$$M_3C \rightarrow M_3C+M_7C_3 \rightarrow M_3C+M_7C_3+M_2C+M_{23}C_6 \rightarrow M_7C_3+M_2C+M_{23}C_6$$

4. DISCUSSION

4.1 Comparison between experiment and theory

Fig. 5 shows a calculation using the Robson and Bhadeshia model [1] compared against experimental data for 3Cr1.5Mo steel. Table III shows how each precipitate is treated. Although the calculations are qualitatively correct, there are some obvious discrepancies. The approach to equilibrium is generally much slower than predicted by the model.

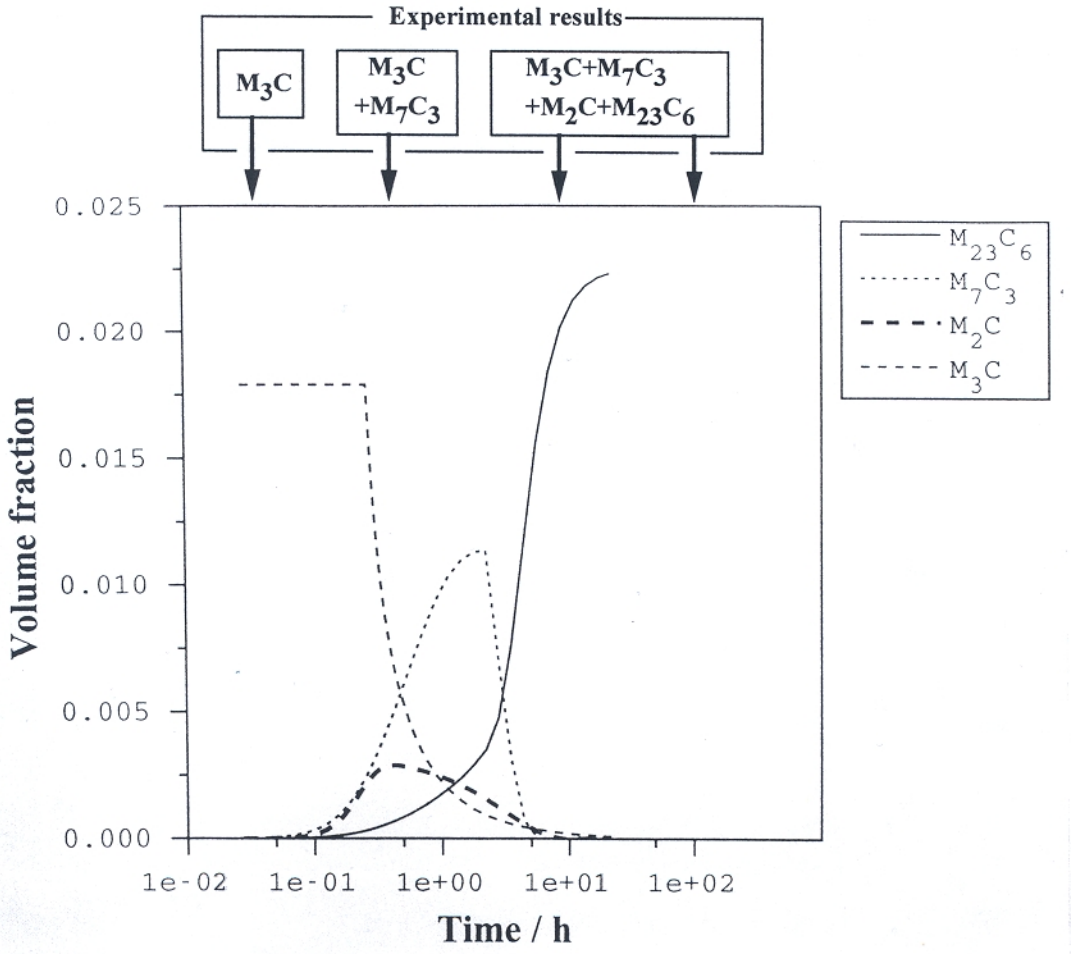

Figure 5: The predicted precipitation sequences [1] along with experimental data for 3Cr1.5Mo steel tempered at 600 °C.

Table III: The main assumptions in the Robson and Bhadeshia model [1].

The microstructural parameters	Diffusion-controlled growth
Constant number of pre-existing M_3C particles	Parabolic law for spherical precipitation
(Constant initial number density of particles)	Lengthening with constant
Constant thickness of M_3C and aspect ratio of M_2C	aspect ratio for needle precipitation
Use mean particle size	Both are controlled only by Cr diffusion
Interfacial energies	

4.2 Difficulty 1: The thickness of M_3C particles

M_3C particles have been assumed to be uniform in size for the calculations presented in Fig. 5, with the particle thickness set to 1 μm, a value which is inconsistent with the measured thickness. Fig. 6 shows the thickness of M_3C on martensitic lath boundaries and within laths, as a function of tempering time at 600 °C. The error bars correspond to two standard deviations. After 10 h of heat treatment, it became difficult to find enough M_3C particles for meaningful measurements with error bars. Because less than 20 particles were measured, the distribution of thicknesses was so small that only the average measured values are plotted in Fig. 6. The size does not seem to change for times less than 10 h. The thickness of particles on lath boundaries was about twice that of those within the laths.

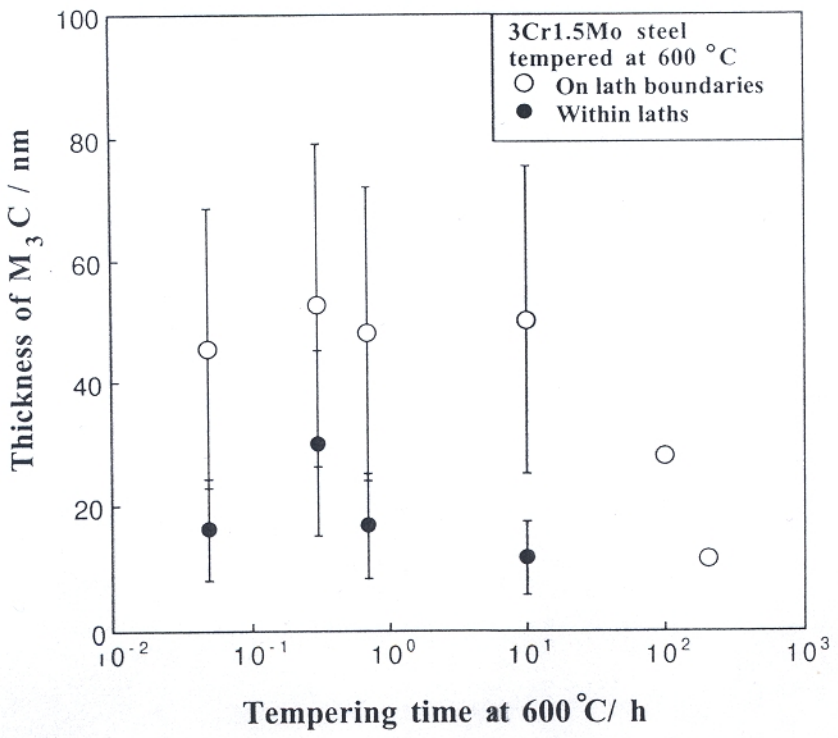

Figure 6: The thickness of M_3C on lath boundaries and within laths as a function of the tempering time at 600 °C.

4.3 Difficulty 2: The number density of M_3C particles

For the purposes of the calculations in Fig. 5, the number density of M_3C particles was assumed to be 5.49×10^{21} m^{-3}, which was assumed to be independent of steel composition in the original work [12]. However, the total volume fraction of M_3C must be a function of the carbon concentration. As emphasized in Fig. 6, the thickness is approximately constant before the dissolution of M_3C, so that the initial number density N_V of M_3C particles must be a function of the carbon concentration. The average measured value of N_V in specimens tempered at 600 °C for times where only M_3C exists was 1.23×10^{21} m^{-3} for 0.1C-3Cr1.5Mo steel. To create an empirical expression for N_V as a function of the carbon concentration, measurements were also made on 0.15C-$2\frac{1}{4}$Cr1Mo steel tempered at 600 °C, in which case $N_V = 2.35 \times 10^{21}$ m^{-3} [13]. If the effect of other alloying elements is neglected, then it is expected that N_V increases with carbon concentration. Therefore, N_V (m^{-3}) was assumed to increase in proportion to the carbon concentration C (wt%) as follows:

$$N_V = 2.23 \times 10^{22} C - 1.0 \times 10^{21} \tag{1}$$

4.4 Difficulty 3: The aspect ratio of M_2C

The aspect ratio (length / width) of M_2C needles was assumed to be constant at 50. However, the measurements indicated values between 10 and 20, so that the aspect ratio was set at 15 for the present work.

4.5 Difficulty 4: Avrami theory

One difficulty in the application of Avrami theory is that the conversion of extended space into real space, necessary to account for impingement, prevents the calculation of anything but the average particle size. Given that the total fraction of precipitates is small, this difficulty can be avoided by neglecting impingement altogether. It should then be possible to estimate size distributions.

4.6 Difficulty 5: Diffusion controlled-growth in a multicomponent steel

The original model treats the growth of all precipitates other than M_3C in terms of the diffusion of chromium alone, with the interface composition given by a tie-line passing through the mean alloy composition ($\overline{c}$). The analysis of diffusion-controlled growth therefore involves just one condition for mass conservation at the interface which is moving with a velocity v:

$$v(c_{Cr}^{\beta\alpha} - c_{Cr}^{\alpha\beta}) = D_{Cr}(\partial c_{Cr}/\partial x)_{x=x^I} \tag{2}$$

where $c_{Cr}^{\beta\alpha}$ and $c_{Cr}^{\alpha\beta}$ are the equilibrium concentrations of chromium in β (precipitate) and α (ferrite) phases respectively, D_{Cr} is the diffusion coefficient of chromium in α phase and $(\partial c_{Cr}/\partial x)_{x=x^I}$ is the chromium concentration gradient in the α phase at the α / β interface.

As emphasized in the classic work of Kirkaldy [14] and Coates [15], this binary treatment is inadequate for a ternary or higher order steels. This is because the diffusion coefficient of

the interstitial solute can be many orders of magnitude greater than that of the substitutional solute. A second mass conservation equation must be simultaneously satisfied:

$$v(c_C^{\beta\alpha} - c_C^{\alpha\beta}) = D_C(\partial c_C/\partial x)_{x=x^I} \tag{3}$$

But to do this and maintain local equilibrium at the moving interface, a tie-line must be chosen which reduces the driving force for carbon diffusion so that the slower moving chromium can keep pace with the carbon. Such a tie-line will not in general pass through $\overline{c}$. Indeed, the tie-line defining the interface compositions will not be constant but will shift towards $\overline{c}$ as precipitation progresses (Fig. 7) [15]. Notice in Fig. 7 that the effective value $\overline{c}'$ of $\overline{c}$ at the point where alloy carbide precipitation begins is the composition of the ferrite after the precipitation of cementite by a paraequilibrium mechanism.

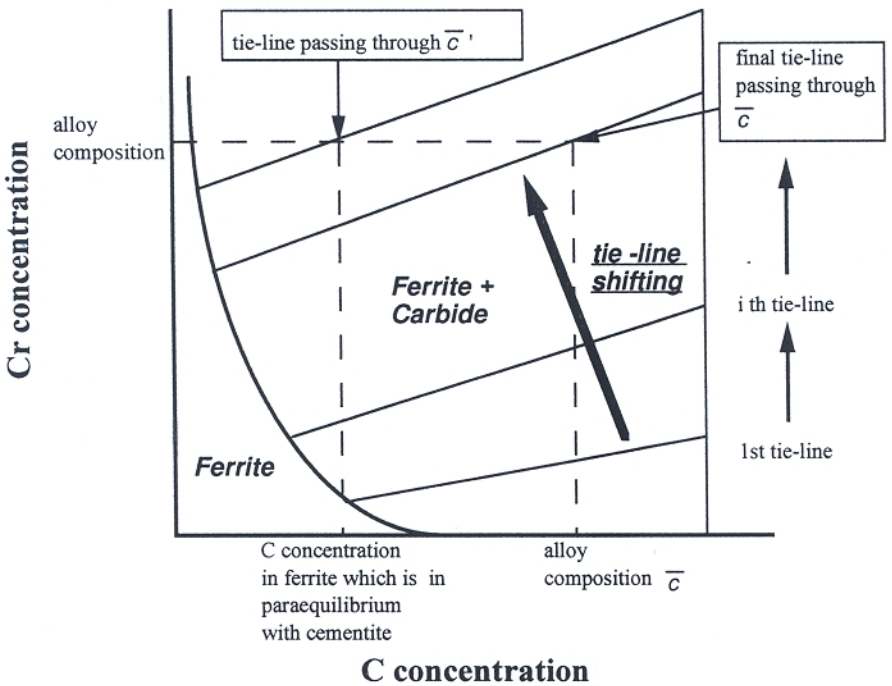

Figure 7: The schematic drawing for tie-line shifting in Fe-Cr-C system.

5. THE MODIFIED MODEL

The measured microstructural parameters used in the modified model are shown in Table IV. Table V shows the comparison of assumptions between the original and modified models. The results for 3Cr1.5Mo are shown in Fig. 8 along with the experimental observations.

Table IV: The measured values used in the modified model

The microstructural parameters	The values in use
Number density of sites for M_3C at 600 °C	1.23×10^{21} m^{-3}
Thickness of M_3C on lath boundaries	5.0×10^{-8} m
Thickness of M_3C on lath boundaries	2.0×10^{-8} m
Aspect ratio for needles of M_2C	15.0

Table V: The comparison of assumptions used in both models.

The original model	The modified model
Based on Avrami theory	Nucleation and growth but no treatment of impingement
Using mean particle size	Particle size distribution due to different nucleation times and growth rates
Cr diffusion-controlled growth	Diffusion-controlled growth in Fe-Cr-C system

Comparison with Fig. 5 shows that the modified model is in better agreement with experimental data. However, M_3C precipitation is still under estimated.

M_3C forms by a paraequilibrium mechanism but the cementite during aging enriches with chromium. The chromium enrichment was calculated in the model using published theory [16]; it stops when the cementite achieves its equilibrium composition. Cementite begins to dissolve when the chromium concentration in ferrite falls below its equilibrium with cementite, as alloy carbides precipitate and consume solute. The diffusion distance for this was assumed to be a mean distance between all particles. A concentration gradient therefore arises between the cementite and alloy carbide. This assumption may not be realistic and the problem needs a more rigorous analysis.

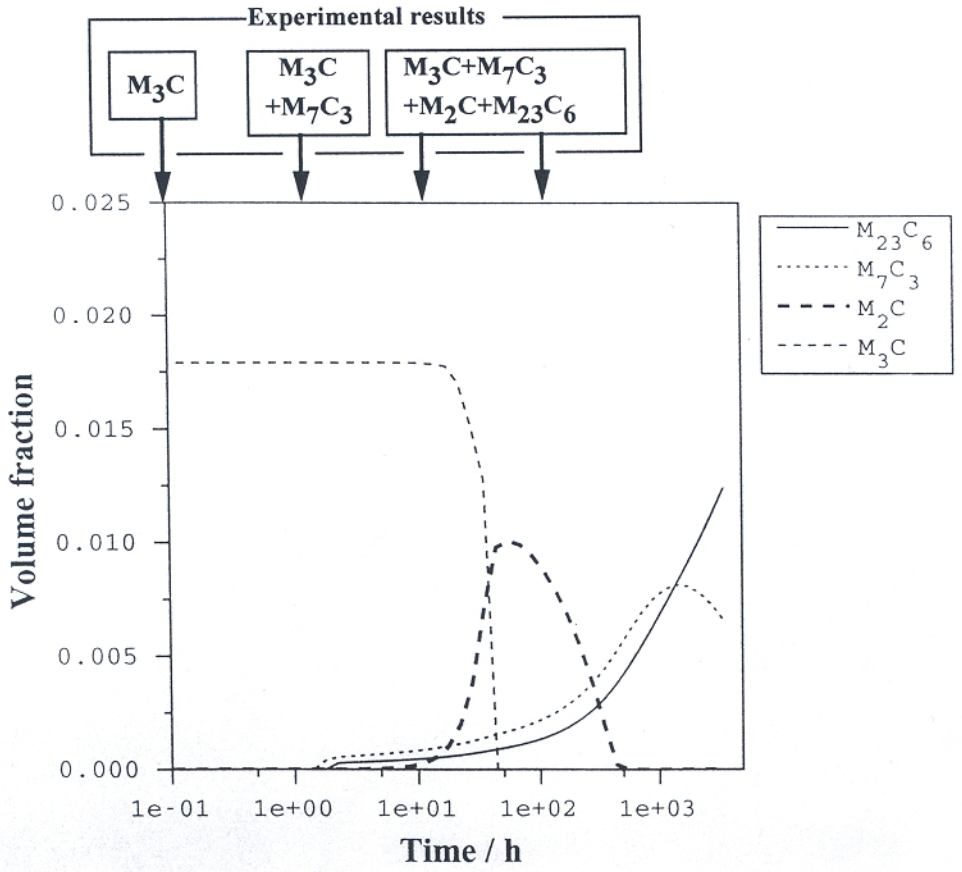

Figure 8: The calculation of multiple precipitation reactions at 600 °C by the modified model for 3Cr1.5Mo steel.

6. CONCLUSIONS

New experimental data have been generated on the precipitation reactions in 3Cr1.5Mo steel which was tempered from a martensitic state. These results indicated a need to modify a theory for the prediction of the kinetics of precipitation reactions. In particular, a multicomponent treatment of the diffusion-controlled-growth of alloy carbides has introduced a proper conservation of mass in the model. The new calculations have been carried out without the Avrami conversion of extended space into real space, a satisfactory approximation given the minute fractions of precipitates involved. The new model shows better agreement with experimental data.

REFERENCE

1) Robson, J. D. and Bhadeshia, H. K. D. H. : *Mat. Sci. Tech.* **13** (1996) 631
2) Robson, J. D. and Bhadeshia, H. K. D. H. : *Mat. Sci. Tech.* **13** (1996) 640
3) Jones, S. J. and Bhadeshia, H. K. D. H. : *Acta. Metall.* **45** (1996) 2911
4) Kolmogorov, A. N. : *Bull. Accad. Sci. USSR Phys. Ser.* **3** (1937) 355
5) Johnson, W. A. and Mehl, R. F. : *Trans. Am. Inst. Min.(Metall.) Engrs.* **135**(1939) 416
6) Avrami, M. : *J. Chem. Phys.* **7** (1939) 1103
7) Avrami, M. : *J. Chem. Phys.* **8** (1940) 212
8) Avrami, M. : *J. Chem. Phys.* **9** (1941) 177
9) Hodson, S. M. : MTDATA-Metallurgical and Thermochemical Databank, National Physical Laboratory, Teddington, U.K.(1989)
10) Ashby, M. F. and Ebeling, R. : *Trans. Metall. Soc. AIME* **236** (1966) 1396
11) Beech, J. and Warrington, D. H. : *J. Iron Steel Inst.* **204** (1966) 460
12) Robson, J. D. : Ph.D. Thesis, University of Cambridge, U.K. (1996)
13) Fujita, N. : Unpublished work, University of Cambridge, U.K. (1997)
14) Kirkaldy, J. S. : *Can. J. Phys.* **36** (1958) 907
15) Coates, D. E. : *Metall. Trans.* **4** (1973) 2313
16) Bhadeshia, H. K. D. H. : *Mat. Sci. Tech.* **5** (1989) 131